Advanced Biomedical Research & Innovation

Research Article

Design and Synthesis of Nano-Sized Polymer Stabilized Hybrid Materials Based on Iron Oxide and Silver Nanoparticles and their Antifungal activity

Pencheva D[1], Bryaskova R[2*], Ismail S[2], Cardoso A[3], Mancheva I[3], Rancheva M[4], Korkova A[4], Stoyanova E[4], Vasileva Y[3], Ivanova Z[5] and Kantardjiev T[5]

Abstract

The high level of resistance of yeast species of the genus *Candida* to antifungal agents used in the practice, defines the scientific interest to investigate the antifungal properties of newly synthesized hybrid materials. The research is directed to find a viable alternative for the treatment of infections caused by the highly resistant *Candida* species. The tested in the experiments nano-sized bimetallic polymer stabilized hibrid materials based on iron oxide and silver nanoparticles (γFe_2O_3/AgNps/PVA), were characterized by different techniques and for the first time tested onto six clinical Candida strains with a predetermined resistance to different antimycotics. The results showed the presence of very strong antifungal activity.

Keywords

Candida; *Antimycotics*; Resistance; Magnetic nanoparticles; Silver nanoparticles

Introduction

Species of the genus *Candida* are the fourth most causative agent of nosocomial bloodstream infections in USA as well as one of the most isolated microorganisms from hospital-acquired infections in Europe [1,2]. Nowadays a tendency for increasing of cases caused by non-albicans *Candida* species resistant toward one or more antifungal agents was observed. Among them *C. glabrata* demonstrated a high degree of resistance to fluconazole and voriconazole and enhance resistance to echinocandins [3-7]. *C. glabrata* is a fungus that unlike other fungi of the genus Candida is not polymorphic (i.e., does not form hyphae or pseudo hyphae) and exists only in the form of blastokonidium. In the beginning, this fungus has been classified to the genus *Torulopsis*, because it does not form hyphae and pseudo hyphae. However, later it has been decided that the formation of pseudo hyphae is not a reliable factor for distinguishing different types of fungi. Therefore, *Torulopsis glabrata* is affiliated to the genus Candida due to the fact that as other Candida strains it also infects the human organism [8]. The main future of *C. glabrata* among other representatives is the presence of haploid genome as well as its biochemical characteristics. For example, *C. glabrata* absorbs only glucose and trehalose in comparison to *C. albicans* that absorb a number of sugars [9].

Candida nivariensis was previously identified as *Candida glabrata*, but on the basis of genetic, culture and biochemical differences, it has been separated and described as a individual species in 2005 [10]. It possesses high resistance to many azole antifungals, including itraconazole, fluconazole, voriconazole. The considerable resistance to flucytosine is described as well [11]. *C. krusei* is an important causative agent of various infections in immunocompromised patients, fungemia, endophthalmitis, endocarditis, arthritis, and oropharyngeal and esophageal candidiasis [12]. A major problem in the treatment of infections caused by *C. krusei* represents the resistance to the fungicidal preparations. There are many reports in the literature, which described the mechanisms of development of resistance towards drug fluconazole [13-16]. Cases of resistance towards itraconazole and caspofungin were also described [17,18]. To overcome the problem of the growing resistance toward different type antimicrobials, hybrid materials containing different metal nanoparticles are the object of scientific research interest in order to investigate their activity towards microorganisms [19-21]. Their effect on the yeast is a challenge because of the eukaryotic cell type system of the strains. It is important to define the exact concentration at which they will exhibit their fungicidal activity without presence of cytotoxic effect on the human cells. The aim of the present investigation is to synthesize novel hybrid materials, which combine the properties of silver and iron based magnetic nanoparticles stabilized by polyvinyl alcohol with high antimicrobial activity and delivery targeting. For this purpose, it is necessary to examine and compare the presence of antifungal activity of the newly synthesized hybrid materials and to determine their minimal fungicidal concentration (MFC) for selected clinical yeast with a predetermined resistance to different antimycotics.

Materials and Methods

Materials

Polyvinyl alcohol (PVA) (Sigma – Aldrich; 87-88% hydrolyzed, Mw = 13000 – 23000 mol^{-1}); silver nitrate (AcrosOrganics); $FeCl_3.6H_2O$ (Sigma-Aldrich); $FeCl_2.4H_2O$ (Sigma-Aldrich); $Fe(NO_3)_3.9H_2O$ (Sigma-Aldrich) were used as received without further purification.

Clinical yeast strains resistant toward one or more antimycotics were involved in the experiment as follow: ***C. krusei 112, C. krusei 8-48, C. krusei 8-126, C. glabrata 0-73, C. glabrata 8-122, C. Nivariensis.***

Methods

- Transmission electron microscopy (TEM) images were recorded on a HR STEM (JEOL JEM 2100). Samples were prepared by placing a drop of the precursor solutions on carbon-coated grids and dried under air at room temperature.
- Dynamic light scattering measurements (DLS) were performed on a NanoBrook 90 plus PALS instrument

***Corresponding author:** Rayna Bryaskova, Department Polymer Engineering, University of Chemical Technology and Metallurgy, Sofia, Bulgaria, E-mail: rbryaskova@uctm.edu

Received: November 09, 2017 **Accepted:** January 17, 2018 **Published:** January 23, 2018

(Brookhaven Instruments Corporation), equipped with a 35 mW red diode laser (l ¼ 660 nm) at a scattering angle of 90.

- UV- Vis absorption spectra were recorded at room temperature in the wavelength range from 200 to 800 nm using Perkin Elmer spectrophotometer.
- IR spectra of the films were recorded in transmittance mode in the range from 400 to 4000 cm^{-1} using Perkin Elmer FTIR.
- XRD analysis is performed on PANalytical- X-ray diffractometers.

Synthesis of silver nanoparticles via thermal reduction using Polyvinyl alcohol (PVA) as a stabilizer

The synthesis of silver nanoparticles stabilized by PVA was performed as reported by Bryaskova et al. [19]. Briefly, five grams of PVA was dissolved in 95 mL deionized water under stirring at 80ºC. Silver nitrate (30 mg) dissolved in 5 mL (water) was added drop-wise under stirring to 95 mL of PVA solution (5%) thus achieving final concentration of silver nitrate in the solution equal to 300 mg/L. The prepared solution was heated for 1 h at 100°C in dark thus leading to the formation of silver nanoparticles (AgNps) stabilized via PVA. The color of the solution was light yellow.

Preparation of γFe_2O_3/AgNps/PVA

First magnetite (Fe_3O_4) nanoparticles in aqueous solution were prepared according to by dissolving 3.25 g $FeCl_3.6H_2O$ and 1.197g $FeCl_2$. $4H_2O$ in 70 ml deoxygenated water [22-24]. Then 7 ml 25% NH_4OH was added drop-wise into solution under vigorous stirring with formation of black precipitate. After sedimenting the precipitate with a permanent magnet, the supernatant was removed by decantation and the precipitate was washed with water several times until the neutral pH of solution. Then 20 ml 2M HNO_3 was added to the black sediment and the mixture was stirred for 10 min. The oxidation of magnetite to maghemite was then performed by addition of 30 ml 0.35M $Fe(NO_3)_3$. The mixture was stirred under reflux for 1h at 100ºC. The color of the solution changed from blue-black to clear reddish-brown. After sedimentation and washing with 2M HNO_3, the reddish yellow sediment was dispersed by adding demineralized water and stirred. The supernatant was collected; the clear, reddish brown supernatant is a hydrosol of Fe_2O_3 nanoparticles, which was mixed with solution of AgNps stabilized with PVA. This sample will be referred as **P1** (product1) in the text. The concentration of the Ag and Fe was established by ICP as 88 mg/L and 5401 mg/L respectively. Then, the solid was dispersed with certain amount of AgNps solution stabilized with PVA and mixed for 1h. The obtained suspension will be referred as **P2** (product 2) in the text. The concentration of the Ag and Fe was established by ICP as 157.5 mg/L and 1989 mg/L respectively. For control, Fe_2O_3 hydrosol mixed with PVA solution was used and this product will be referred as **P3** (product 3) in the text. The concentration of the Fe was established by ICP as 6097 mg/L.

Testing the fungicidal properties of the γFe_2O_3/AgNps/PVA hybrid materials

For evaluation of the fungicidal activity of the materials the Minimal Fungicidal Concentration (MFC) was determined. This was achieved by the method of macro dilution in a final volume of 1 ml. Materials **P1** and **P2** are tested initially from outgoing dilution 1:100 by two-fold serial dilutions up to 1:1600, but the MFC was not achieved. Therefore, the subsequent tests were started from a dilution of 1:1000 and two-fold dilutions are conducted up to 1:32000. The product P3 was tested without initial dilution as the subsequent two-fold dilutions were performed to 1:1024. As a diluent was used injection water. To each dilution of the material, standardized inoculum of the test strain containing 10^5-10^6 CFU/ml of the respective species of yeast was added. After incubation at 32.5 ± 2.5°C for 18-24 h, seeding was performed from each dilution by the surface agar method on plates with Sabouraud agar. The results are reported in advance at 24 hours, and final on the 5th day after incubation at 32.5 ± 2.5°C.

Results and Discussion

To prepare γFe_2O_3/AgNps/PVA bimetallic hybrid materials for targeting delivery and in vivo applications, surface modification of naked iron oxide nanoparticles with AgNps/PVA hybrid materials possessing antimicrobial properties was performed. For this purpose, initially PVA stabilized silver nanoparticles was synthesized by boiling the PVA solution at 100ºC for 60 min in the presence of $AgNO_3$ as a precursor of silver ions [19]. The UV-vis spectroscopy analysis confirms the formation of well-defined silver nanoparticles with appearance of peak at 420 nm. The TEM analysis also demonstrated the formation of spherical and homogenous distributed silver nanoparticles with particles diameter from 5.0 to 6.0 nm (Figure 1 a-b).

Then, Fe_3O_4 nanoparticles were synthesized applying wet-chemical coprecipitation of ferrous and ferric ions in an aqueous solution upon addition of ammonium hydroxide. The stability of thus prepared iron nanoparticles is however critical and oxidation to more stable maghemite γFe_2O_3 was performed. The main problem of those naked magnetic nanoparticles is their ability to aggregate. To overcome this problem, γFe_2O_3 nanoparticles were coated with biocompatible and non-toxic PVA with included silver nanoparticles. Uncharged polymers such as PVA or PEO are known to adsorb nonspecifically on oxide surfaces. The interaction with the surface results from hydrogen bonding between polar functional groups of the polymer and hydroxylated and protonated surface sides of the oxide [25].

Two different γFe_2O_3/AgNps/PVA bimetallic hybrid materials were prepared: 1) hydrosol of γFe_2O_3 stabilized with AgNps/PVA, referred as **P1** and 2) sediment of γFe_2O_3 stabilized with AgNp/PVA, referred as **P2**. The morphology and the size of thus prepared γFe_2O_3/AgNps/PVA products were determined by TEM analysis. TEM images of the first product (**P1**) showed the presence of individual magnetic/silver nanoparticles with diameter ranging between 5-10 nm (Figure 2a). The same observation was made for the second product (**P2**), with the presence of individual magnetic/silver nanoparticles, which however tend to form aggregated clusters (Figure 2c). The selected area electron diffraction pattern (SAED) of γFe_2O_3/AgNps/PVA materials indicates that they are nanocrystalline. The patterns of SAED are indexed as (200), (313), (317), (426), (513) and (517) reflections, which correspond to tetragonal crystal stucture of γFe_2O_3 with lattice constant: a=8.346, c=25.034 according to JCPDS (89-5894) (Figure 2 b, d).

The average hydrodynamic diameter (Dh) and particles size distribution of the bimetallic γFe_2O_3/AgNps/PVA nanoparticles was determined by DLS. The average hydrodynamic diameter was Dh=75 nm with a polydispersity of 0.15 for **P1**, and Dh=115 nm and polydispersity of 0.17 for **P2** respectively. The naked γFe_2O_3 showed significantly higher hydrodynamic diameter Dh = 720 nm, which indicates that AgNps/PVA coating of magnetic nanoparticles improved the overall stability of iron oxide nanoparticles in aqueous

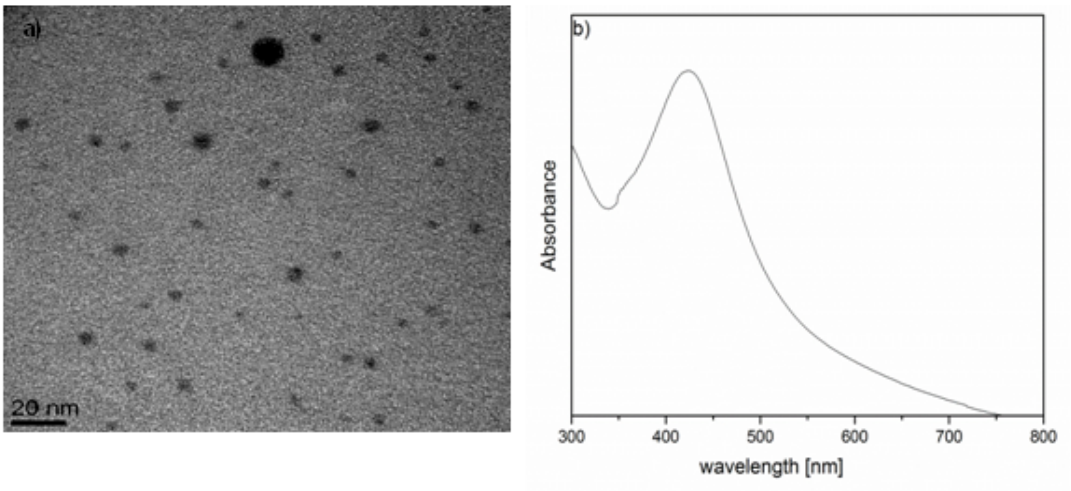

Figure 1: a) TEM image of AgNps/PVA nanoparticles and b) UV-vis analysis of AgNps/PVA nanoparticles.

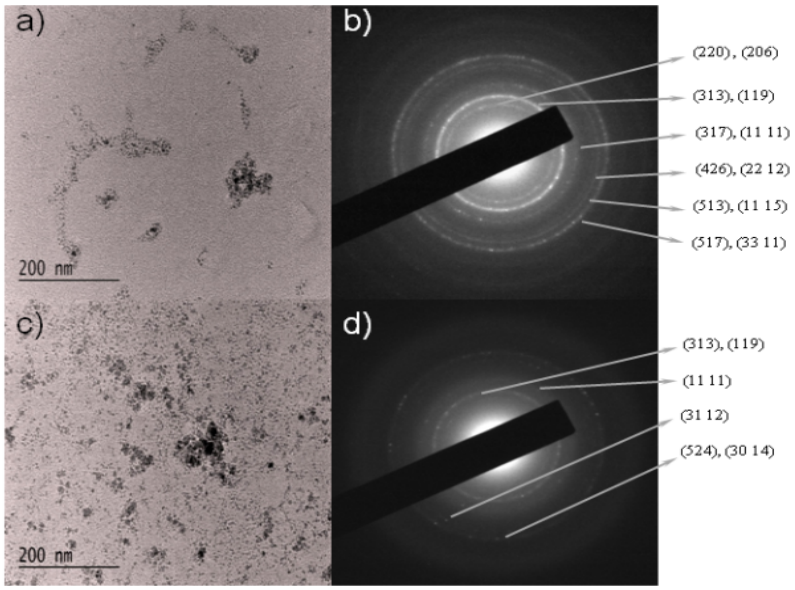

Figure 2: TEM pictures and SAED analysis of γFe_2O_3/AgNps/PVA products: (a-b) for P1 and (c-d) for P2

solution shown by significantly reducing the size of the nanoparticles thus preventing to some extent the formation of large aggregates (Figure 3).

The observed difference between the hydrodynamic diameter and those observed by TEM is due to the formation of small clusters between particles in aqueous solution.

FTIR analysis of the synthesized γFe_2O_3/AgNps/PVA product (P2) showed the presence of all-characteristic for PVA signals at 3300 cm^{-1}, which is due to the O-H vibrations of hydroxyl groups originated from the main PVA chain. The peaks at 1326 cm^{-1} are characteristic for the C-H deformation vibration in PVA and the absorption peak at 1000-1100 cm^{-1} can be assigned to the C-O stretching and O-H bending vibrations arising from the PVA chain. The presence of magnetic iron oxide nanoparticles can be seen by two strong absorption bands at around 634 and 566 cm^{-1} (Figure 4).

XRD analysis

For the the γFe_2O_3/ PVA/AgNps products (P2), diffraction peaks at 30.36 (220), 35.77 (313), 43.35 (400), 53.76 (422), 57.16 (511), and 62.98 (440) were observed which are ascribed to the normal structure of γFe_2O_3, and confirm the results of SEAD analysis [26]. Additionally, not very intensive peaks at 38.1° (111), 44.09° (200), 64.36° (220), 77.29° (311), were observed as well, which are referred to the standard data of Ag. Evidently, no other impurities peaks are detected (Figure 5). Moreover, the X-ray fluorescent (XRF) results confirm the existence of γ-Fe_2O_3 and presence of Ag with determined mass percentage of Ag - 1.5% and for Fe – 96.5% respectively (Figure 5).

Fungicidal activity

To test the fungicidal activity of thus prepared γFe_2O_3/ AgNps/ PVA bimetallic nanoparticles, ***six clinical strains with proven***

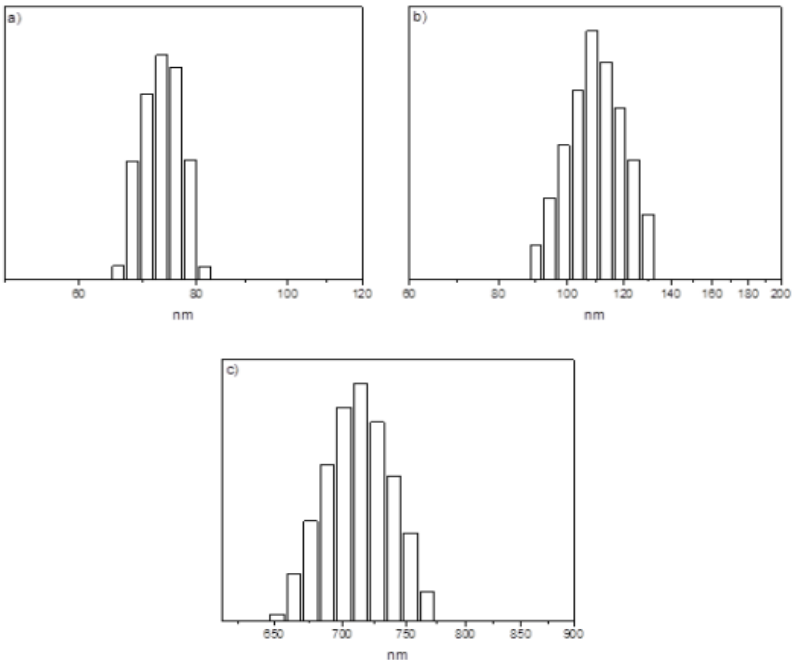

Figure 3: DLS analysis of γFe_2O_3/AgNps/PVA products and γFe_2O_3 nanoparticles a) P1; b) P2 and c) pure γFe_2O_3.

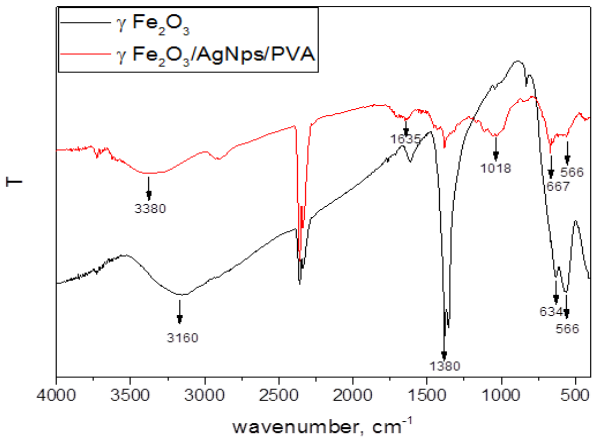

Figure 4: FTIR spectra of γFe_2O_3 and γFe_2O_3/ PVA/AgNps (P2)

resistance toward one or more antimycotics were involved in the experiment as follow: C. krusei 112, C. krusei 8-48, C. krusei 8-126, C. glabrata 0-73, C. glabrata 8-122, and C. nivariensis. Their antimycotical resistance determined using commercial kit ATB Fungus 3 ***is shown in Table 1.*** The minimal fungicidal concentration (MFC) of the tested products towards six clinical Candida strains were determined by surface agar method and the results are shown in Table 2. ***The presence of fungicidal activity of all synthesized products (P1-P3) onto the tested clinical yeast strains was observed. As expected, taking into account the difference into the type of the yeasts, which belong to various Candida strains, difference in MFC of the products was established.***

The MFC for the strain C. krusei 8-126 are significantly higher for the P1 and P2 in comparison to the MFC of other strains Candida. This is indicative for the higher resistance of the strains compared to all tested yeasts (Figure 6 a). *C. krusei* demonstrated ability to grow in a medium with a lack of vitamins, temperature maximum of 43-45°C, production of phospholipases and proteases, ability to attach to the surfaces of the host and formation of hyphae. It is established that *C. krusei* is attached easier towards inert substances, than to the epithelial cells of the buccal mucosa [12]. These specific characteristics of the strain probably determined the higher resistance of the tested strain. The lowest values for MFC were observed for *C. nivariensis* 383, which determined it as the most sensitive strain from all tested Candida strains (Figure 6 b).

The MFC of **P1** for strain ***C. krusei 112 was determined at*** 0.04 mg/L ***Ag*** and 2.71 mg/L Fe ***concentrations***. For strains ***C. krusei 8-48 and C. glabrata 0-73, the MFC is higher in comparison to the rest of the strains – at concentration of AgNps 0.09*** mg/L and 5.401 mg/L of Fe nanoparticles. The lower concentration was determined for ***C. glabrata 8-122***-0.02 mg/L Ag and 1.4 mg/L Fe concentrations.

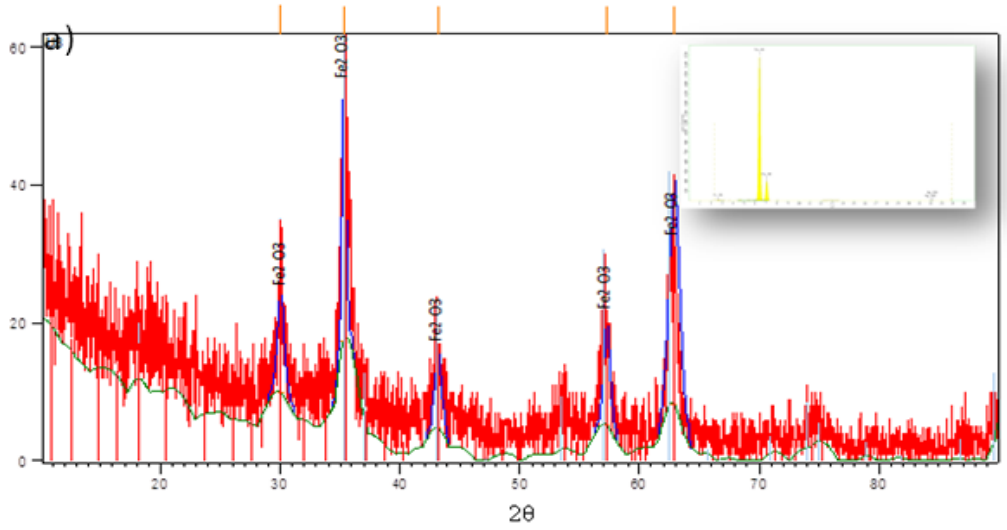

Figure 5: XRD and XRF analysis of γFe_2O_3/ PVA/AgNps.

Table 1: Antimycotical resistance of the tested clinical yeast strains.

№	Clinical strain	Antimycotical resistance
1.	*C. krusei* 8-112	FCA, ITR
2.	*C. krusei* 8-48	FLU, MCZ
3.	*C.krusei 8-126*	ITR
4.	*C. glabrata* 0-73	FLU
5.	*C. glabrata 8-122*	FCA, ITR
6.	*C. nivariensis* 383	FLU, VOR, ITR

Legend: Fluconazole (FCA), Itraconazole (ITR) and Voriconazole (VRC), using commercial kit ATB Fungus 3 "Bio Merieux and Miconazole (MCZ).

Table 2: MFC of the products determined for six clinical fungi strains.

Clinical fungi strains	P1		P 2		P 3	
	Ag mg/L	Fe mg/L	Ag mg/L	Fe mg/L	Ag mg/L	Fe mg/L
C. krusei 112	0.04	2.7	0.1	1.0	0	1524
C. krusei 8-48	0.09	5.4	0.1	1.0	0	3048
C. krusei 8-126	0.2	13.5	0.2	2.5	0	762
C. glabrata 0-73	0.09	5.4	0.04	0.5	0	1524
C. glabrata 8-122	0.02	1.4	0.04	0.5	0	762
C. nivariensis 383	0.01	0.7	0.04	0.5	0	95

The MFC of **P2** for strains ***C. krusei 112 and C. krusei 8-48 was higher than the strains C. glabrata 0-73 and C. glabrata 8-122:*** 0.1 mg/L Ag and 1.0 mg/L Fe concentrations. For the strains ***C. glabrata 0-73, C. glabrata 8-122 and C. nivariensis no growth was observed at 0.04 mg/L Ag and 0.5 mg/L Fe concentrations. The observed deviations in MFC for both the products are a result of the observed difference in their size and this determined their antifungicidal activity.***

P3 containing only γFe_2O_3 nanoparticles showed the presence of fungicidal activity for all tested strains but at concentration much higher than those products containing AgNps. MFC for the strain C. krusei 8-48 was 3048 mg/L. For the strains *C. krusei* 112 and *C. glabrata* 0-73, MFC was 1524 mg/L. Only for *C. krusei* 8-126 and *C. glabrata* 8-122, MFC was lower respectively 762 mg/L (Figure 6 c, d, e, f).

The presence of antimicrobial activity of magnetic nanoparticles based on Fe^0 or Fe_3O_4 is reported in the literature [27,28]. It is supposed that several oxido-reduction reactions take place that produce very reactive oxygen species because of Fenton reaction or Haber-Weiss cycle, thus iron in magnetite nanoparticles is fully oxidized to maghemite (γ-Fe_2O_3) via a series of reactions [27]. This causes oxidative stress to bacterial cells, and bacterial cell death, respectively. In contrast, fully oxidized maghemite is relatively stable in culture medium and do not generate significant cytotoxicity or genotoxicity *in vitro* due to the absence of electronic or ionic transfer [29,30].

Conclusion

Bimetallic nanoparticles based on magnetic iron oxide and silver nanoparticles (γFe_2O_3/ AgNps) stabilized by PVA were synthesized and characterized. The results indicate a synergistic action at the combination of silver and iron nanoparticles in the hybrid materials when tested onto selected six clinical strains of yeast. The presence of only iron nanoparticles showed a fungicidal activity

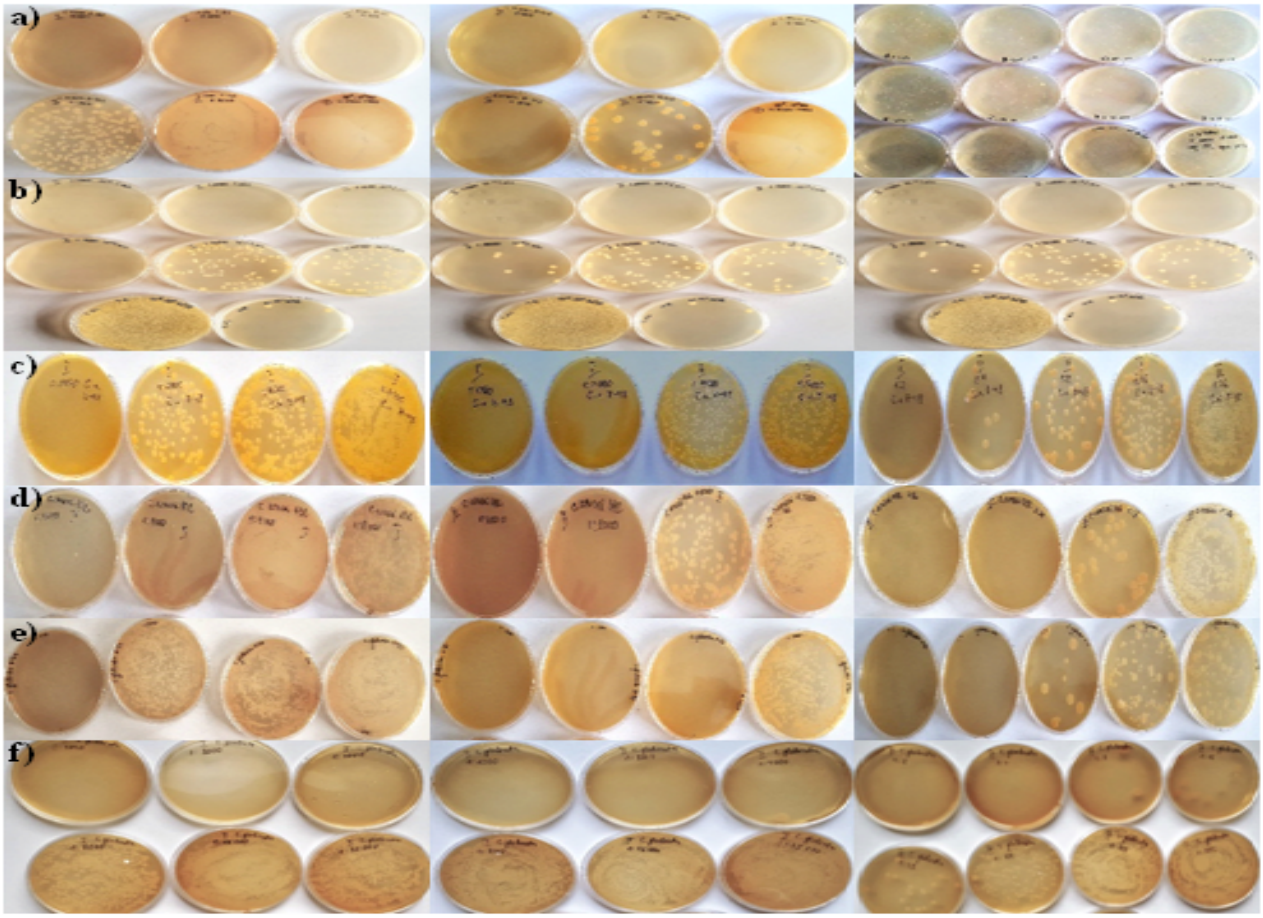

Figure 6: The MFC of P1,P2 and P3.

at exceeding concentration compared to their content in hybrid materials containing both silver and magnetic nanoparticles. These results indicate that thus prepared bimetallic γFe_2O_3/AgNps/PVA nanoparticles can find potential application for target delivery under magnetic field in biomedical area.

The study is a part of the scope of the project Biomedicine and Molecular Bioscience COST Action BM 1309.

References

1. Wisplinghoff H, Bischoff T, Tallent SM, Seifert H, Wenzel RP, et al. (2004) Nosocomial bloodstream infections in US hospitals: analysis of 24,179 cases from a prospective nationwide surveillance study. Clin Infect Dis 39: 309-317.
2. Point prevalence survey of health care associated infections and antimicrobial use in European acute care hospitals (2013) Stockholm: ECDC.
3. Lockhart SR, Iqbal N, Cleveland AA (2012) Species identification and antifungal susceptibility testing of Candida bloodstream isolates from population-based surveillance studies in two U.S. cities from 2008 to 2011. J Clin Microbiol 50: 3435-3442.
4. Pfaller MA, Messer SA, Hollis RJ, Boyken L, Tendolkar S, et al (2009) Variation in susceptibility of bloodstream isolates of Candida glabrata to fluconazole according to patient age and geographic location in the United States in 2001 to 2007. J Clin Microbiol 47: 3185-3190.
5. Pfaller MA, Diekema DJ, Gibbs DL (2010) Results from the ARTEMIS DISK Global Antifungal Surveillance Study, 1997 to 2007: a 10.5-Year Analysis of Susceptibilities of *Candida* Species to Fluconazole and Voriconazole as Determined by CLSI Standardized Disk Diffusion. J Clin Microbiol 48: 1366-1377.
6. Vallabhaneni S, Cleveland A, Farley M (2015) Epidemiology and Risk Factors for Echinocandin Nonsusceptible Candida glabrata Bloodstream Infections: Data From a Large Multisite Population-Based Candidemia Surveillance Program, 2008-2014. Open Forum Infect Dis 2: ofv163.
7. Alexander BD, Johnson MD, Pfeiffer CD, Jimenez-Ortigosa C, Catania J, et al (2013) Increasing echinocandin resistance in Candida glabrata: clinical failure correlates with presence of FKS mutations and elevated minimum inhibitory concentrations. Clin Infect Dis 56: 1724-1732.
8. Silva S, Negri M, Henriques M (2012) Candida glabrata, Candida parapsilosis and Candida tropicalis: biology, epidemiology, pathogenicity and antifungal resistance. FEMS Microbiol Rev 36: 288-305.
9. Fidel PL, Vazquez JJA, and Sobel JD (1999) Candida glabrata: Review of Epidemiology, Pathogenesis, and Clinical Disease with Comparison to C. Albicans. Clin Microbiol Rev 12: 80-96.
10. Alcoba-Flórez J, Méndez-Álvarez S, Cano J, Guarro J, Pérez-Roth et al. (2005) Phenotypic and Molecular Characterization of Candida nivariensis sp. nov., a Possible New Opportunistic Fungus. J Clin Microbiol 43: 4107-4111.
11. Borman A, Petch R, Linton CJ, Palmer MD, Bridge PD et al. (2008) Candida nivariensis, an Emerging Pathogenic Fungus with Multidrug Resistance to Antifungal Agents. J Clin Microbiol 46: 933-938.
12. Yuthika H, Samaranayake LP (1994) Candida krusei: biology, epidemiology, pathogenicity and clinical manifestations of an emerging pathogen. J Med Microbiol 41: 295-310.
13. Orozco AS (1998) Mechanism of Fluconazole Resistance in Candida krusei. Antimicrob Agents Chemother 42: 2645-2649.

14. Erwin L (2009) Abc1p is a multidrug efflux transporter that tips the balance in favor of innate azole resistance in Candida krusei. Antimicrob Agents Chemother 53: 354-369.

15. Guinea J (2006) Fluconazole resistance mechanisms in Candida krusei: the contribution of efflux-pumps. Med Mycol 44: 575-578.

16. Berjan C, Clancy CJ, Nguyen MH (1999) Antifungal resistance in non-albicans Candida species. Drug resistance updates 2: 9-14.

17. Venkateswarlu K (1996) Reduced accumulation of drug in Candida krusei accounts for itraconazole resistance. Antimicrob Agents Chemother 40: 2443-2446.

18. Morgan H, Staab JF, Marr KA (2006) Emergence of a Candida krusei isolate with reduced susceptibility to caspofungin during therapy. Antimicrob Agents Chemother 50: 2522-2524.

19. Bryaskova R, Pencheva D, Kale GM, Lad U, Kantardjiev T, et al. (2010) Synthesis, characterisation and antibacterial activity of PVA/TEOS/Ag-Np hybrid thin films. J Colloid Interface Sci 349: 77-85.

20. Prucek R, Tuček J, Kilianová M, Panáček A, Kvítek L, et al. (2011) The targeted antibacterial and antifungal properties of magnetic nanocomposite of iron oxide and silver nanoparticles. Biomaterials 32: 4704-4713.

21. Kooti M, Saiahi S, Motamedi H (2013) Fabrication of silver-coated cobalt ferrite nanocomposite and the study of its antibacterial activity. J Magn Magn Mater 333: 138-143.

22. Bee A, Massart R (1995) Synthesis of very fine maghemite particles. J Magn Magn Mater 149: 6-9.

23. Van Ewijk CA, Vroege GJ, Philipse AP (1999) Convenient preparation methods for magnetic colloids. J.Magn Magn Mater 201: 31-33.

24. Chastellain M, Petri A, Hofmann H (2004) Particle size investigations of a multistep synthesis of PVA coated superparamagnetic nanoparticles. J Colloid Interface Sci 278: 353-360.

25. Lee LT, Somasundaran P (1989) Adsorption of polyacrylamide on oxide minerals. Langmuir 5: 854-860.

26. Ni YH, Ge XW, Zhang ZC, Ye Q (2002) Fabrication and Characterization of the Plate-Shaped γ-Fe2O3Nanocrystals. Chem Mater 14: 1048 - 1051.

27. Auffan M, Rose J, Wiesner MR, Bottero JY (2009) Chemical stability of metallic nanoparticles: A parameter controlling their potential cellular toxicity in vitro. Environ Pollut 157: 1127-1133.

28. Arakha M, Pal S, Samantarrai D, Panigrahi TK, Mallick BC, et al. (2015) Antimicrobial activity of iron oxide nanoparticle upon modulation of nanoparticle-bacteria interface. Sci Rep 5: 14813.

29. Auffan M, Achouak W, Rose J, Chane´ac C, Waite DT, et al. (2008) Relation between the redox state of ironbased nanoparticles and their cytotoxicity towards Escherichia coli. Environ Sci Technol 42: 6730-6735.

30. Limbach LK, Wick P, Manser P, Grass RN, Bruinink A, et al. (2007) Exposure of engineered nanoparticles to human lung epithelial cells: influence of chemical composition and catalytic activity on oxidative stress. Environ Sci Technol 41: 4158-4163.

Author Affiliations

Top

[1]*Bul Bio-National Centre of Infectious and Parasitic Diseases, Sofia, Bulgaria*

[2]*Department Polymer Engineering, University of Chemical Technology and Metallurgy, Sofia, Bulgaria*

[3]*Department of Biology, Sofia University St. Kliment Ohridski, Sofia, Bulgaria*

[4]*Department of Medicine, Sofia University St. Kliment Ohridski, Sofia, Bulgaria*

[5]*National Centre of Infectious and Parasitic Diseases, Sofia, Bulgaria*